

# PCCP

Accepted Manuscript



This is an *Accepted Manuscript*, which has been through the Royal Society of Chemistry peer review process and has been accepted for publication.

*Accepted Manuscripts* are published online shortly after acceptance, before technical editing, formatting and proof reading. Using this free service, authors can make their results available to the community, in citable form, before we publish the edited article. We will replace this *Accepted Manuscript* with the edited and formatted *Advance Article* as soon as it is available.

You can find more information about *Accepted Manuscripts* in the [Information for Authors](#).

Please note that technical editing may introduce minor changes to the text and/or graphics, which may alter content. The journal's standard [Terms & Conditions](#) and the [Ethical guidelines](#) still apply. In no event shall the Royal Society of Chemistry be held responsible for any errors or omissions in this *Accepted Manuscript* or any consequences arising from the use of any information it contains.

# New *ab initio* potential energy surfaces for the ro-vibrational excitation of OH( $X^2\Pi$ ) by He

Yulia Kalugina\*

LOMC - UMR 6294, CNRS-Université du Havre,  
25 rue Philippe Lebon, BP 540, 76058, Le Havre and  
Tomsk State University, 36 Lenin av., Tomsk 634050, Russia

François Lique†

LOMC - UMR 6294, CNRS-Université du Havre,  
25 rue Philippe Lebon, BP 540, 76058, Le Havre, France

Sarantos Marinakis‡

School of Biological and Chemical Sciences, Queen Mary University of London,  
Joseph Priestley Building, Mile End Road, London E1 4NS, UK

(Dated: May 4, 2014)

We present a new set of three-dimensional potential energy surfaces (PES) for the OH( $X^2\Pi$ )-He van der Waals system, which explicitly takes into account the OH vibrational motion. *Ab initio* calculations of the OH-He PES were carried out using the open-shell single- and double-excitation coupled cluster approach with non-iterative perturbational treatment of triple excitations [RCCSD(T)]. The augmented correlation-consistent aug-cc-pVXZ ( $X = Q, 5, 6$ ) basis sets were employed, and the energies obtained were then extrapolated to the complete basis set (CBS) limit. Integral and differential cross sections (ICS and DCS), and thermal rate constants for the rotational excitation in OH+He collisions were calculated using the new PES, and compared with available experimental results. Experimental and theoretical results were found to be in a very good agreement. The newly constructed PES reproduces the available experimental results for OH( $X^2\Pi, v = 0, 1$ )+He collisions better than the previously available two-dimensional PESs, which were constructed using a fixed OH bond distance. Our work provides the first RCCSD(T) PES for future anticipated experiments in OH( $X^2\Pi, v \geq 0$ ) + He collisions.

## I. INTRODUCTION

Collisions of OH molecules with rare gases, such as Ar and He, have emerged as paradigms in the field of inelastic and elastic collisions of open-shell species (see ref. [1] and references therein). This is largely a result of its experimental and theoretical accessibility. In addition, OH radical is a key species in the troposphere, combustion and photochemistry.

The OH radical was one of the first molecules to be observed in the interstellar medium (ISM) [2], and it is one of the most abundant diatomic species in molecular clouds. OH has been widely observed in interstellar medium through rotational and  $\Lambda$ -doublet transitions [3]. Astronomical OH maser action associated with the  $\Lambda$ -doublet transfer transitions has also been observed. In masers involving the upper spin-orbit state of the OH ground electronic state, the required population inversion is possibly induced by H<sub>2</sub>O photodissociation [4]. For maser action involving the lower spin-orbit state of the OH ground electronic state, the required population inversion is possibly due to inelastic OH collisions which preferentially excite the upper  $\Lambda$ -doublet levels [4].

In addition, the Herschel Space Observatory have recently collected new OH emission data from young stellar objects [5], from protoplanetary disks [6] or from low- and intermediate-mass protostars [7]. The OH radical is a key species in the water chemistry network of star-forming regions, because its presence is tightly related to the formation and destruction of water. As collisions compete with radiation to excite interstellar molecule, it is crucial to have an accurate knowledge of the OH excitation due to collisions with the most abundant species in these molecular clouds. Accurate OH-He rate coefficients (using He as a model for H<sub>2</sub> [8]) may then allow accurate determination of OH abundance in the ISM.

In this work, we compute a new set of *ab initio* PESs for the ro-vibrational excitation of OH( $^2\Pi$ ) by He. Despite accurate potential energy surfaces have been already published, there is a lack of OH-He PESs that take into account the OH vibrational motion accurately. Such PESs are highly needed in order to interpret past and future experiments on the inelastic scattering of OH with He. Indeed, it is common to prepare OH molecules in excited vibrational state, e.g. from HNO<sub>3</sub> photodissociation [9, 10]. This paper is organized as follows: Section II presents a review on previous work on OH(X)-He. Section III describes the *ab initio* calculations, and the analytical fit of the PES obtained. In Section III, a comparison between experimental and theoretical inelastic ICS, DCS and rate coefficients is described. Conclusions

\* kalugina@phys.tsu.ru

† francois.lique@univ-lehavre.fr

‡ s.marinakis@qmul.ac.uk

drawn from this comparison, and future outlook are also presented.

## II. PREVIOUS WORK ON OH(X)-HE

About two decades ago, Schreel *et al.* [11] reported for the first time state-to-state integral cross sections (ICS) for OH( $X^2\Pi_{3/2}, v = 0$ ) + He rotational energy transfer (RET) collisions at a collision energy ( $E_{\text{col}}$ ) of  $394\text{ cm}^{-1}$ . That work stimulated theoretical interest, and the first *ab initio* intermolecular potential energy surfaces (PES) was constructed by Esposti *et al.* [12] using the coupled electron pair approximation (CEPA). Esposti *et al.* also calculated close-coupling cross sections for OH + He collisions, and they found a good agreement with the measurements by Schreel *et al.* Schreel *et al.* [13] went on to measure steric asymmetry factors at the same collision energy. Their main conclusion was that rotational excitation is preferential for collisions at the H-end than the O-end of the OH molecule.

Lee *et al.* [14] constructed new PESs for the OH( $X^2\Pi$ )/OH( $X^2\Sigma^+$ )-He systems using restricted open-shell coupled cluster (RCCSD(T)) level of theory, and the triple-zeta correlation-consistent basis set (aug-cc-pVTZ) augmented with an additional ( $3s3p2d2f1g$ ) set of bond functions. In their calculations, the OH bond length was set equal to  $0.96966\text{ \AA}$  ( $1.8324 a_0$ ), which is the experimentally determined equilibrium distance [15]. As it will be discussed later, this was the most used PES for OH(X,A)-He so far.

Approximately a decade later, Hickson *et al.* [9] measured rate coefficients,  $k_{\Lambda}$ , for  $\Lambda$ -doublet changing OH( $X^2\Pi_{3/2}, v = 1, j = 6.5$ ) + He collisions at room temperature. In a later work, Hickson *et al.* [10] presented RET rate coefficients,  $k_{\text{RET}}$ , for OH( $X^2\Pi_{3/2}, v = 1, j = 1.5, 3.5, 4.5, 6.5, 7.5, 8.5$ ) + He collisions at room temperature. Although RET rate coefficients depend to a small degree on the  $\Lambda$ -doublet level, this possible difference was not examined in their analysis. A direct comparison of these experimental rate coefficients with theory was not possible due to lack of calculated rate coefficients for that system. Han *et al.* [16] were able to experimentally observe the OH(X,A)-He van der Waals complexes using laser excitation of the  $A^2\Sigma^+ - X^2\Pi$  transition. From the van der Waals complex unresolved band, which showed a redshift of  $1.6\text{ cm}^{-1}$  from the OH monomer band, Han *et al.* were able to identify the complex features as scattering resonances. The bound state calculations by Lee *et al.* [14], yielded bond dissociation energies,  $D'_0 = 6.04\text{ cm}^{-1}$  for the OH(X)-He state, and  $D'_0 = 7.12\text{ cm}^{-1}$  for the OH(A)-He state. These theoretical values give a difference of  $D'_0 - D''_0 = 1.08\text{ cm}^{-1}$ , which is only around  $0.5\text{ cm}^{-1}$  lower than the experimental value of  $1.6\text{ cm}^{-1}$ .

Marinakis *et al.* [17] combined one-colour polarization spectroscopy (PS) experiments and exact close-coupling quantum mechanical calculations to measure state-to-state OH( $X^2\Pi_{3/2}, v = 0, j = 1.5 - 6.5$ ) + He elastic de-

polarization rate coefficients at room temperature. With the term elastic depolarization, we refer to collisions that change the projection of the total rotational angular momentum,  $m_j$ , but not  $j$ . In those experiments, the elastic depolarization coefficient,  $k_{\text{DEP}}$ , was inferred from the equation

$$k_{\text{DEP}} = k_{\text{PS}} - k_{\text{POP}} = k_{\text{PS}} - k_{\text{RET}} - k_{\Lambda} \quad (1)$$

where  $k_{\text{PS}}$  is the PS signal loss rate coefficient, and  $k_{\text{POP}}$  is the coefficient for the collisional removal of population from the prepared quantum state. The term  $k_{\text{RET}}$  denotes the sum of all RET rate constants for transitions out of the prepared quantum state. Thus, in order to determine  $k_{\text{DEP}}$ , a prior knowledge of  $k_{\text{RET}}$  and  $k_{\Lambda}$  is necessary. For this reason, Marinakis *et al.* calculated these coefficients using the PES constructed by Lee *et al.* [14], and inferred that only weak elastic depolarization occurs in these collisions. In a parallel work, Kłos *et al.* [18] calculated rate coefficients up to 500 K for OH(X) + He collisions using the PES by Lee *et al.*. They also presented values of cross sections at  $394\text{ cm}^{-1}$  that were in a good agreement with the experimental cross sections obtained by Schreel *et al.* [11].

The  $k_{\text{PS}}$  in one-colour PS experiments mentioned previously [17] were dependent not only on the evolution of the OH(X) rotational angular momentum (RAM) polarization but also, albeit to a small extent, on the evolution of the OH(A) RAM polarization. In order to study exclusively the evolution of the ground-state OH(X) RAM polarization, Paterson *et al.* [19] used two-colour PS experiments. The experimentally measured two-colour  $k_{\text{PS}}$  was for the most of the rotational levels smaller than the calculated  $k_{\text{POP}}$ , leading to negative  $k_{\text{DEP}}$  through eqn (1). These PS experiments stimulated further theoretical interest, and Dagdigian *et al.* [20] modified HIBRIDON scattering code [21] in order to directly calculate elastic depolarization cross sections through a tensor cross sections formalism instead of using eqn (1). There was a good agreement with the experimental results for loss of alignment for the highest rotational levels studied. In most cases, however, the positive values of theoretical  $k_{\text{DEP}}$  suggested that either there was a systematic underestimate of the experimental  $k_{\text{PS}}$  or the OH(X)-He PES by Lee *et al.* overestimated the  $k_{\text{POP}}$ .

Due to significant interest of OH in cold molecules collisions, Sawyer *et al.* [22] measured total (elastic and inelastic) cross sections of collisions between magnetically trapped OH(X) radicals and He beams at  $E_{\text{col}}$  between 60 and  $230\text{ cm}^{-1}$ . The measured cross sections could not be reproduced by theoretical calculations by Pavlovic *et al.* [23]. Subsequent, independent measurements of field-free OH(X) + He collisions by Kirste *et al.* [24] at  $E_{\text{col}}$  between 120 and  $400\text{ cm}^{-1}$  were in good agreement with calculations using the PES by Lee *et al.*. This lead Kirste *et al.* to infer that the trap loss measured by Sawyer *et al.* was dominated by elastic and not inelastic scattering. In order to test the experimental results in Ref. [24], Gubbels *et al.* [25] presented

new PESs for the OH(X)–He system. Initially, they constructed new two-dimensional (2D) PESs by using an augmented quintuple-zeta correlation-consistent basis set (aug-cc-pV5Z) plus the  $(3s3p2d1f1g)$  midbond functions, which is larger than the aug-cc-pVTZ employed by Lee *et al.* Gubbels *et al.* preferred to use the vibrationally-averaged OH bond distance of  $r_0 = 1.8502 a_0$  than the equilibrium distance,  $r_e$ , which was employed by Lee *et al.* Indeed, as already discussed in other systems [26], a better description of the intermolecular potential is obtained by fixing the molecular distance at its average value in the ground vibrational level rather than at the equilibrium distance.

Gubbels *et al.* noticed that the newly constructed PESs offered only a small improvement in the agreement with the experimental data by Kirste *et al.* For this reason, Gubbels *et al.* constructed three-dimensional (3D) PESs using aug-cc-pVTZ basis set and midbond orbitals with geometry-dependent exponents to calculate and successfully fit the variation of the potential with OH bond lengths between  $0.75$  and  $3.0 a_0$ . Gubbels *et al.* constructed an adiabatic 2D potential

$$V_{\text{ad}}(R, \theta) = \langle 0' | \hat{H}'_{\text{OH}} | 0' \rangle - \langle 0 | \hat{H}_{\text{OH}} | 0 \rangle \quad (2)$$

where  $\hat{H}'_{\text{OH}} = \hat{H}_{\text{OH}} + V(R, \theta, r)$ ,  $\hat{H}_{\text{OH}}$  is the corresponding Hamiltonian for the OH monomer,  $V(R, \theta, r)$  is the calculated RCCSD(T)/aug-cc-pVTZ PES, and  $0$  denotes the ground vibrational state. Using this adiabatic 2D PES, the agreement between theoretical and experimental data was significantly improved showing the importance of taking into account the vibration of the diatomic molecules. However, the PESs of Gubbels *et al.* were specifically tailored for interpreting OH( $v = 0$ )–He experiments and the strategy they used to take into account the vibration of the OH molecule may not be as accurate for describing collision of OH in vibrationally excited states as it is for the ground state.

The PES by Lee *et al.* was again tested by Dagdigan *et al.* in ref. [27], where they compared exact quantum scattering calculations of He-OH diffusion coefficients with available experimental data at room temperature [28], and at temperatures between 218 and 318 K [29]. The theoretical value of He-OH diffusion coefficient at room temperature was within the uncertainty limits of ref. [28]. The theoretical values at temperatures between 218 and 318 K, however, laid above the uncertainty limits of ref. [29]. Sarma *et al.* [1] obtained differential cross sections (DCSs) for OH( $X^2\Pi, v = 0, j = 1.5f$ ) + He collisions at  $E_{\text{col}} = 460 \text{ cm}^{-1}$ . Unfortunately, DCSs for only three final rotational levels ( $^2\Pi_{3/2}, j = 1.5e$ ,  $^2\Pi_{3/2}, j = 2.5e$ , and  $^2\Pi_{1/2}, j = 0.5e$ ) in the OH ground vibrational state were obtained in their proof-of-principle measurements. The limited number of DCSs obtained did not allow for a thorough test of the PES by Lee *et al.* The agreement between theoretical and experimental DCS was in general satisfactory, except for scattering in the most forward directions, where the experimental background subtraction procedure is least reliable [1].

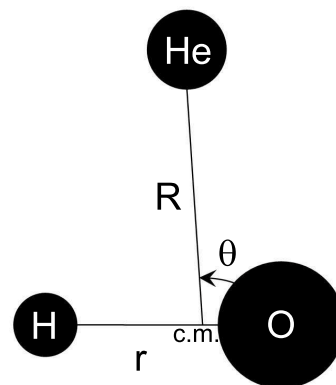


FIG. 1: Jacobi coordinate system of the OH–He complex.

### III. CONSTRUCTION AND FIT OF THE OH(X)-HE PES

#### A. *Ab initio* calculations

The open-shell OH molecule has a  $^2\Pi$  electronic ground state. The electronic orbital angular momentum and the electron spin have well-defined projections of  $\Lambda = \pm 1$  and  $\Sigma = \pm 1/2$ , onto the internuclear axis. Because of this, there are two spin-orbit manifolds; the lower-energy  $^2\Pi_{3/2}$  with  $|\Omega| = |\Lambda + \Sigma| = 3/2$  (labelled  $F_1$ ), and the higher-energy  $^2\Pi_{1/2}$  with  $|\Omega| = 1/2$  (labelled  $F_2$ ). Each rotational level  $j$  is split into two close lying  $\Lambda$ -doublet levels labelled  $e$  (total parity  $+(-1)^{j-1/2}$ ) and  $f$  (total parity  $-(-1)^{j-1/2}$ ) [30]. When the OH( $X^2\Pi$ ) radical interacts with a spherical structureless target, the doubly-degenerate  $\Pi$  electronic state is split into two states, one of  $A'$  symmetry and one of  $A''$  symmetry. These two states correspond to the singly occupied  $\pi$  orbital lying in, or perpendicular to, the triatomic plane, respectively.

The Jacobi coordinate system used in this work to represent the coordinates is shown in Fig. 1. The center of coordinates is placed in the OH center of mass (c.m.), and the vector  $\mathbf{R}$  connects the OH c.m. with the He atom. The rotation of OH molecule is defined by the  $\theta$  angle. We note that the convention for the orientation of  $\theta$  in this work, is the opposite to the orientation of  $\theta_{\text{old}}$  used in all previous studies. These two angles are connected through the equation:  $\theta = 180^\circ - \theta_{\text{old}}$ . The calculations were performed for five OH bond lengths  $r = [1.5, 1.65, 1.85, 2.1, 2.4] a_0$  which allows us to take into account vibrational motion of OH molecule up to  $v = 2$  (see Fig. 2).

*Ab initio* calculations of the PESs of OH( $X^2\Pi$ )-He van der Waals complexes being in  $A'$  and  $A''$  electronic states were carried out at the partially spin-restricted coupled cluster with single, double and perturbative triple excitations [RCCSD(T)] [31, 32] level of theory using MOLPRO 2010 package [33]. In order to determine the interaction potential,  $V(R, \theta, r)$ , the basis set superposition error (BSSE) was corrected at all geometries using the

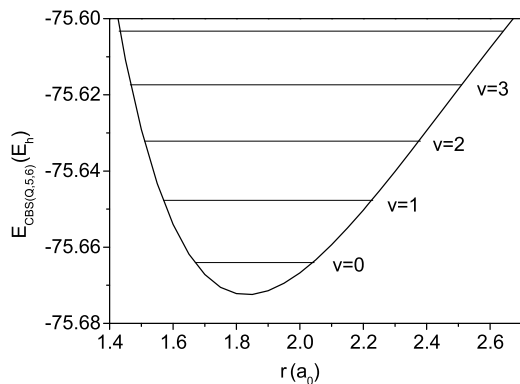


FIG. 2: Vibrational states of OH ( $X^2\Pi_{3/2}$ ) molecule obtained from the potential energy calculated at the RCCSD(T)/CBS(Q,5,6) level.

Boys and Bernardi counterpoise scheme [34]:

$$V(R, \theta, r) = E_{\text{OH-He}}(R, \theta, r) - E_{\text{OH}}(R, \theta, r) - E_{\text{He}}(R, \theta, r) \quad (3)$$

where the energies of the OH and He monomers are computed in a full basis set of the complex.

To achieve a good description of the charge-overlap effects the calculations were performed in a rather large augmented correlation-consistent basis sets aug-cc-pVXZ ( $X = Q, 5, 6$ ) [35]. Then, the energies were extrapolated to the Complete Basis Set (CBS) limit using the following scheme [36]:

$$E_X = E_{\text{CBS}} + Ae^{-(X-1)} + Be^{-(X-1)^2}, \quad (4)$$

where  $X$  is the cardinal number of the aug-cc-pVXZ basis set,  $E_X$  is the energy corresponding to aug-cc-pVXZ basis set,  $E_{\text{CBS}}$  is the energy extrapolated to CBS limit,  $A$  and  $B$  are the parameters to adjust. The calculations were carried out for  $\theta$  angle values from  $0^\circ$  to  $180^\circ$  in steps of  $10^\circ$ .  $R$ -distances were varied from  $3.0$  to  $50.0 a_0$ , yielding 42 points for each angular orientation. Overall 3990 single point energies were calculated for each state of OH-He complex ( $A'$  and  $A''$ ).

### B. Analytical representation and features of the potential energy surfaces

In the present work, the analytical expression employed for the interaction potential  $V(R, \theta, r)$  of both  $A'$  and  $A''$  surfaces has the following form [37]:

$$V(R, \theta, r) = \sum_{n=1}^N \sum_{l=1}^L B_{l,n}(R)(r - r_e)^{n-1} d_{m0}^{l+m-1}(\cos(\theta)), \quad (5)$$

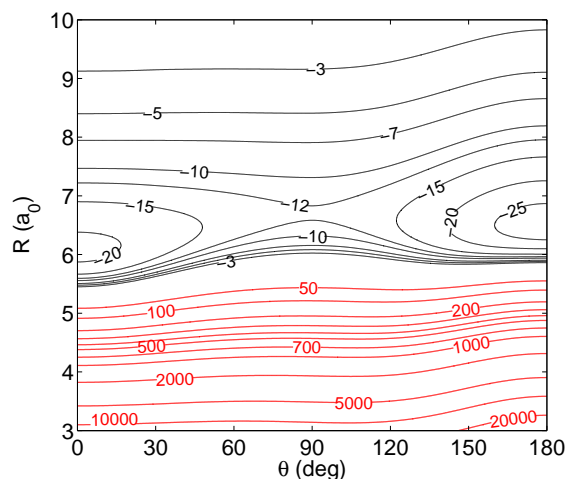
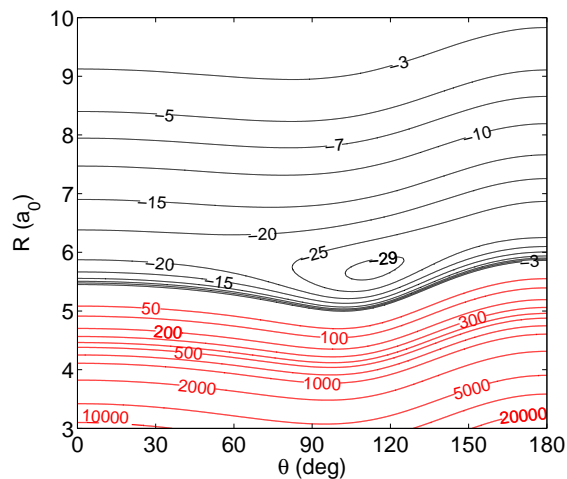


FIG. 3: (Color online) Contour plots of the He-OH(X)  $A'$  (upper panel) and  $A''$  (lower panel) PES for  $r_e = 1.8324 a_0$ . Energy is in  $\text{cm}^{-1}$ . Red contour lines represent repulsive interaction energies.

where

$$B_{l,n}(R) = e^{-a_{l,n}(R - R_{l,n}^{(0)})} \left( \sum_{i=0}^2 b_{l,n}^{(i)} R^i \right) - \frac{1}{2} \left( 1 + \tanh \frac{R - R_{l,n}^{(1)}}{R_{l,n}^{\text{ref}}} \right) \sum_{j=6,8,10} \frac{c_{l,n}^{(j)}}{R^j}. \quad (6)$$

The basis functions  $d_{m0}^{l+m-1}(\cos(\theta))$  are Wigner rotation functions,  $N$  is the total number of  $r$ -distances, and  $L$  is the total number of angles.

Two-dimensional cuts of the  $A'$  and  $A''$  PES for  $r = r_e$  are shown in Fig. 3. The minimum of  $V_{A'}(R, \theta, r_e = 1.8324 a_0)$  is  $-29.80 \text{ cm}^{-1}$  at  $(R = 5.70 a_0, \theta = 112.8^\circ)$ , and of  $V_{A''}(R, \theta, r_e)$  is  $-27.38 \text{ cm}^{-1}$  at  $(R = 6.53 a_0, \theta = 180.0^\circ)$ . These values are in good agreement with the minima obtained by Lee *et al.* [14] of  $-30.02 \text{ cm}^{-1}$  at  $(R = 5.69 a_0, \theta = 111.4^\circ)$  for  $A'$  state, and of  $-27.06 \text{ cm}^{-1}$

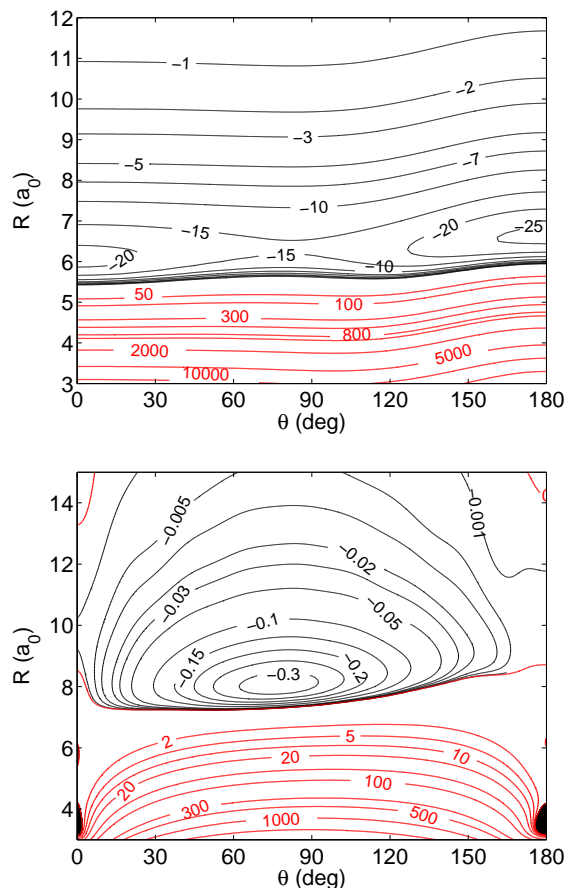


FIG. 4: (Color online) Contour plots of OH(X)-He  $V_{\text{sum}}$  (upper panel), and  $V_{\text{diff}}$  (lower panel) potentials from this work. Energy is in  $\text{cm}^{-1}$ . Red contour lines represent repulsive interaction energies.

at  $(R = 6.54 a_0, \theta = 180.0^\circ)$  for  $A''$  state. The minima obtained from this work at  $r_0 = 1.8502 a_0$  for  $A'$  ( $E = -29.78 \text{ cm}^{-1}$  at  $R = 5.69 a_0, \theta = 111.9^\circ$ ) and  $A''$  ( $E = -27.21 \text{ cm}^{-1}$  at  $R = 6.55 a_0, \theta = 180.0^\circ$ ) are also in good agreement with the minima obtained by Gubbels *et al.* [25] for  $A'$  ( $E = -29.8 \text{ cm}^{-1}$  at  $R = 5.69 a_0, \theta = 111.3^\circ$ ), and for  $A''$  ( $E = -27.1 \text{ cm}^{-1}$  at  $R = 6.56 a_0, \theta = 180.0^\circ$ ).

Previous studies [38] have shown that averaging of the PES over corresponding vibrational level  $v$  leads to a better agreement with experimental results. The newly constructed PES, which takes into account the stretching of the OH molecule, can be averaged over any vibrational state up to  $v = 2$ . The averaging is done using the following formula:

$$V_v(R, \theta) = \langle v(r) | V(R, \theta, r) | v(r) \rangle \quad (7)$$

The OH vibrational wave function  $|v(r)\rangle$  was evaluated using discrete variable representation (DVR) method [39] from *ab initio* calculations of the OH potential function using RCCSD(T)/CBS(Q,5,6) level of theory. The global minimum of the  $A'$  potential averaged over  $v = 0$  is  $-29.63 \text{ cm}^{-1}$  at  $(R = 5.69 a_0, \theta = 110.7^\circ)$  and of the  $A''$

potential also averaged over  $v = 0$  is  $-26.09 \text{ cm}^{-1}$  at  $(R = 6.62 a_0, \theta = 180.0^\circ)$ .

In the scattering calculations, it is more convenient [40] to use the average

$$V_{\text{sum}} = \frac{1}{2} (V_{A''} + V_{A'}) \quad (8)$$

and the half-difference

$$V_{\text{diff}} = \frac{1}{2} (V_{A''} - V_{A'}) \quad (9)$$

of these two potential energy surfaces. In the pure Hund's case (a) limit,  $V_{\text{sum}}$  is responsible for inducing inelastic collisions within a given spin-orbit manifold, and  $V_{\text{diff}}$  for inducing inelastic collisions between the two ( $\Omega = 1/2$ ) and ( $\Omega = 3/2$ ) spin-orbit manifolds. The plots of  $V_{\text{sum}}$  and  $V_{\text{diff}}$  averaged over the ground vibrational state  $v = 0$  are presented in Fig. 4.

#### IV. DISCUSSION

In order to test the newly constructed PES with available experimental data, close-coupling quantum scattering calculations were performed. The close-coupling calculations were carried out using HIBRIDON program [21], which provided integral and differential cross sections. Thermal rate coefficients were obtained by integration of the integral cross sections over a Boltzmann distribution of relative translational energies.

The OH rotation, spin-orbit coupling and  $\Lambda$ -doublet splitting were taken into account, using for  $v = 0$  the OH rotation constant  $B = 18.5487 \text{ cm}^{-1}$ , the spin-orbit coupling constant  $A = -139.21 \text{ cm}^{-1}$ , and  $\Lambda$ -doubling parameters  $p = 0.235 \text{ cm}^{-1}$  and  $q = -0.0391 \text{ cm}^{-1}$  [41]. For  $v = 1$ , the OH rotation constant  $B = 17.82392 \text{ cm}^{-1}$ , the spin-orbit coupling constant  $A = -139.321 \text{ cm}^{-1}$ , and  $\Lambda$ -doubling parameters  $p = 0.224677 \text{ cm}^{-1}$  and  $q = -0.0369394 \text{ cm}^{-1}$  [42] were employed. In the scattering calculations reported here, the hyperfine structure of OH(X) was not taken into account, and the value of the spin-orbit constant was assumed to be independent of the OH-He intermolecular separation. The latter approximation is commonly employed in scattering calculations because of the moderate-to-large intermolecular separations at typical collision energies. The calculations were performed for collision energies up to  $2500 \text{ cm}^{-1}$ , and included OH rotational levels up to  $j = 12$ .

The values of the theoretical integral cross sections obtained using the newly constructed PES for  $v = 0$ , and the PES by Lee *et al.* are compared with the experimental results by Kirste *et al.* [24] in Fig. 5. As shown in Fig. 5, the vibrationally averaged PES reproduces the experimental results significantly better than the previous 2D PESs. Similar results were obtained by Gubbels *et al.* using their averaged potential. Therefore, using a vibrationally-averaged PES is necessary for better agreement with experimental data.

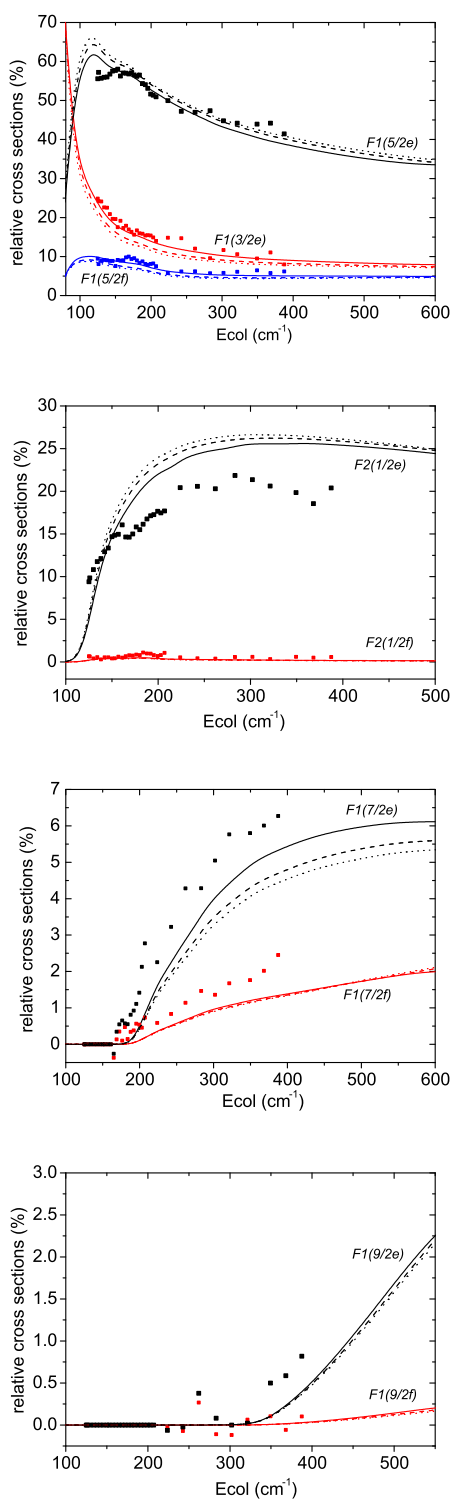


FIG. 5: Relative state-to-state inelastic scattering cross sections for spin-orbit conserving ( $F_1 \rightarrow F_1$ ), and spin-orbit changing ( $F_1 \rightarrow F_2$ ) transitions out of  $j = 1.5f$  level. Squares - experimental values [24]; solid line - present calculations with an averaged PES for  $v = 0$ ; dashed line - present calculations with 2D potential for  $r = r_0$ ; dotted line - theoretical calculations from ref. [18].

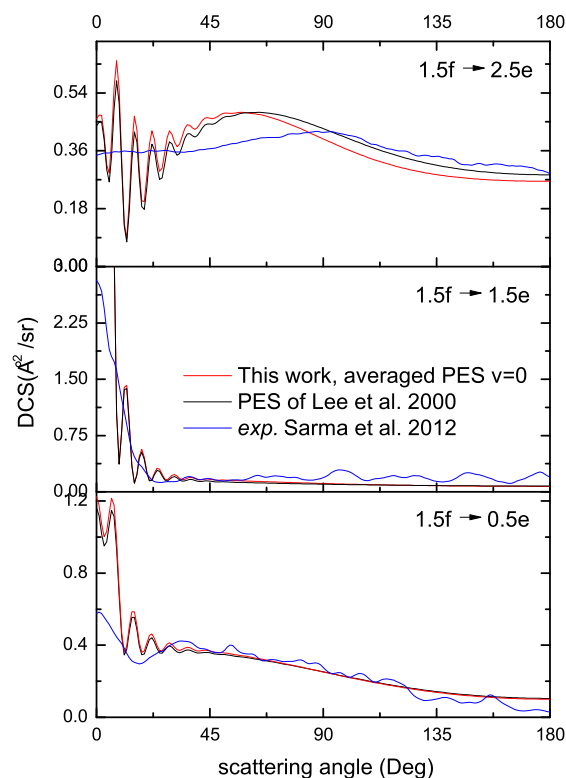


FIG. 6: Comparison between experimental and theoretical differential cross sections (DCS) for transitions out of  $\text{OH}(X^2\Pi_{3/2}, v = 0, j = 1.5f) + \text{He}$  at  $E_{\text{col}} = 460 \text{ cm}^{-1}$ . The theoretical results obtained using the newly constructed PES are from this work. The experimental data and the theoretical results obtained using the PES by Lee *et al.* [14] are from ref. [1].

A comparison between the values of differential cross sections for  $\text{OH}(X^2\Pi_{3/2}, v = 0, j = 1.5f) + \text{He}$  collisions measured by Sarma *et al.* [1] at  $E_{\text{col}} = 460 \text{ cm}^{-1}$  and the theoretical calculations is shown in Fig. 6. The newly constructed PES gives very similar DCSs to those obtained using the PES by Lee *et al.*. Thus, the differences of these two PESs at  $460 \text{ cm}^{-1}$  are not significant as one could have guessed by observing the similarities between the ICSs at high collision energies in Fig. 5. Further measurements of DCS at lower collision energies may provide a more sensitive test of the PES.

We have also calculated the RET,  $k_{\text{RET}}$ , and  $\Lambda$  transfer,  $k_{\Lambda}$ , rate coefficients at  $T = 298 \text{ K}$  in order to further assess the quality of the present PESs by comparing results with the experimental values of refs. [9] and [10] obtained for the first excited vibrational state  $v = 1$ . Rate coefficients  $k_{\Lambda}$  are calculated within  $F_1$  state for transitions between  $e$  and  $f$  levels (for instance, rates for  $j = 1.5e$  to  $j' = 1.5f$  transitions). Rate coefficient  $k_{\text{RET}}$  is the sum of rate coefficients for all possible transitions

TABLE I: Rate constants (in  $10^{-10} \text{ cm}^3 \text{ s}^{-1}$ ) for RET,  $k_{\text{RET}}$ , for  $\Lambda$ -doublet transfer,  $k_{\Lambda}$ , for OH( $^2\Pi_{3/2}$ ) rotational states  $j = 1.5$  to  $j = 6.5$ , at temperature of 298 K.

rate constant	J = 1.5	J = 2.5	J = 3.5	J = 4.5	J = 5.5	J = 6.5
$v = 0$						
$k_{\text{RET}}$ (theory (2D-PES) <sup>a</sup> , $e/f$ )	0.841/1.28	1.45/1.33	1.61/1.31	1.51/1.23	1.33/1.12	1.00/0.953
$k_{\text{RET}}$ (theory (3D-PES) <sup>b</sup> , $e/f$ )	0.866/1.29	1.49/1.33	1.65/1.31	1.56/1.23	1.38/1.14	1.14/1.07
$k_{\Lambda}$ (theory (2D-PES) <sup>a</sup> , $e \rightarrow f, f \rightarrow e$ )	0.125/0.125	0.0988/0.0989	0.0797/0.0798	0.0601/0.0603	0.0455/0.0458	0.0350/0.0352
$k_{\Lambda}$ (theory (3D-PES) <sup>b</sup> , $e \rightarrow f, f \rightarrow e$ )	0.147/0.147	0.118/0.118	0.0969/0.971	0.0748/0.0751	0.0579/0.0583	0.0453/0.0457
$v = 1$						
$k_{\text{RET}}$ (exp) <sup>c</sup>	$1.45 \pm 0.2$	...	$2.0 \pm 0.2$	$1.2 \pm 0.1$	...	$1.1 \pm 0.1$
$k_{\text{RET}}$ (theory (3D-PES) <sup>d</sup> , $e/f$ ) <sup>b</sup>	0.99/1.42	1.56/1.45	1.72/1.42	1.64/1.33	1.47/1.24	1.29/1.14
$k_{\Lambda}$ (exp) <sup>e</sup>	...	...	...	...	...	$0.1 \pm 0.1$
$k_{\Lambda}$ (theory (3D-PES) <sup>d</sup> , $e \rightarrow f, f \rightarrow e$ )	0.134/0.134	0.104/0.104	0.084/0.084	0.064/0.064	0.050/0.050	0.039/0.039

<sup>a</sup>From Marinakis *et al.* [17].

<sup>b</sup>This work, calculations with averaged potential for  $v = 0$ .

<sup>c</sup>From Hickson *et al.* [10].

<sup>d</sup>This work, calculations with averaged potential for  $v = 1$ .

<sup>e</sup>From Hickson *et al.* [9].

out of the corresponding level.

The values of the rate coefficients are reported in Table I. The new theoretical OH( $v = 1$ ) + He rate coefficients from this work reproduce well the available experimental results. The  $k_{\text{RET}}$  values for OH( $v = 0$ ) + He collisions from this work are quite similar to the theoretical calculations in ref. [17] at low rotational levels, but are somewhat higher at high rotational levels. The OH( $v = 0$ ) + He  $k_{\Lambda}$  values from this work are systematically higher than those in ref. [17]. Comparing our theoretical data for  $v = 0$  and  $v = 1$ , we note that the  $k_{\text{RET}}$  values are higher in the ground vibrational state, but the  $k_{\Lambda}$  values are higher in the first excited vibrational state. Thus, as shown in Table I, there are observable vibrational effects on the values of inelastic rate coefficients. These effects can be explained by taking into account the difference in the rotational energy spacings across the two vibrational states, and the increased anisotropy in  $v = 1$  because of the increased averaged OH intramolecular distance. The difference in the vibrational dependence of  $k_{\Lambda}$  and  $k_{\text{RET}}$  may arise because of the difference in the matrix elements involved and because, as discussed in ref. [20], the  $\Lambda$ -doublet changing transitions take place via long-range collisions.

In summary, the quality of the new, full dimensional OH(X)-He PES is verified by comparing with previous experimental and theoretical data for OH(X,  $v = 0, 1$ ) + He collisions. The importance of accurate description of

the OH vibrational motion in the van der Waals complex is demonstrated. Such an effect has also been seen in H + D<sub>2</sub> inelastic collisions [43]. The new PES is shown to be accurate enough for further use in calculation of state-to-state rate coefficients for astrophysical applications and for studying dynamics of excited vibrational states of OH in the OH(X)-He system. In addition, new OH(X) + He scattering experiments will be soon started within the HYDRIDES project [44]. In these experiments, inelastic rate coefficients for OH(X) collisions at low temperatures will be measured. Finally, the newly constructed PES may also be used for providing rotational energy transfer coefficients not only within a specific vibrational state but also across different vibrational states.

## ACKNOWLEDGEMENTS

Y. K. and F. L. greatly acknowledge the financial support of ANR project ‘HYDRIDES’. The *ab initio* and dynamical calculations were carried out using HPC resources of SKIF-Cyberia supercomputer (Tomsk State University). S. M. acknowledges Prof. McKendrick (Heriot-Watt) for introducing him into OH collisions. We acknowledge Dr van de Meerakker for kindly providing the experimental data points for Fig. 5.

- [1] G. Sarma, S. Marinakis, J. J. ter Meulen, D. H. Parker, and K. G. McKendrick, *Nat. Chem.* **4**, 985 (2012).  
 [2] S. Weinreb, A. H. Barrett, M. L. Meeks, and J. C. Henry, *Nature (London)* **200**, 829 (1963).  
 [3] J. M. Brown and A. Carrington, *Rotational Spectroscopy of Diatomic Molecules* (Cambridge University Press, Cambridge, 2003).

- [4] P. Andresen, *A&A* **154**, 42 (1986).  
 [5] S. F. Wampfler, G. J. Herczeg, S. Bruderer, A. O. Benz, E. F. van Dishoeck, L. E. Kristensen, R. Visser, S. D. Doty, M. Melchior, T. A. van Kempen, U. A. Yildiz, C. Dedes, J. R. Goicoechea, A. Baudry, G. Melnick, R. Bachiller, M. Benedettini, E. Bergin, P. Bjerkeli, G. A. Blake, S. Bontemps, J. Braine, P. Caselli, J. Cer-

- nicharo, C. Codella, F. Daniel, A. M. di Giorgio, C. Dominik, P. Encrenaz, M. Fich, A. Fuente, T. Giannini, T. de Graauw, F. Helmich, F. Herpin, M. R. Hogerheijde, T. Jacq, D. Johnstone, J. K. Jørgensen, B. Larsson, D. Lis, R. Liseau, M. Marseille, C. McCoey, D. Neufeld, B. Nisini, M. Olberg, B. Parise, J. C. Pearson, R. Plume, C. Risacher, J. Santiago-García, P. Saraceno, R. Shipman, M. Tafalla, F. F. S. van der Tak, F. Wyrowski, P. Roelfsema, W. Jellema, P. Dieleman, E. Caux, and J. Stutzki, *A&A* **521**, L36 (2010).
- [6] D. Fedele, S. Bruderer, E. F. van Dishoeck, J. Carr, G. J. Herczeg, C. Salyk, N. J. Evans, J. Bouwman, G. Meeus, T. Henning, J. Green, J. R. Najita, and M. Güdel, *A&A* **559**, A77 (2013).
- [7] S. F. Wampfler, S. Bruderer, A. Karska, G. J. Herczeg, E. F. van Dishoeck, L. E. Kristensen, J. R. Goicoechea, A. O. Benz, S. D. Doty, C. McCoey, A. Baudry, T. Giannini, and B. Larsson, *A&A* **552**, A56 (2013).
- [8] E. Roueff and F. Lique, *Chem. Rev.* **113**, 8906 (2013).
- [9] K. M. Hickson, C. M. Sadowski, and I. W. M. Smith, *J. Phys. Chem. A* **106**, 8442 (2002).
- [10] K. M. Hickson, C. M. Sadowski, and I. W. M. Smith, *Phys. Chem. Chem. Phys.* **4**, 5613 (2002).
- [11] K. Schreel, J. Schleipen, A. Eppink, and J. J. ter Meulen, *J. Chem. Phys.* **99**, 8713 (1993).
- [12] A. Degli Esposti, A. Berning, and H.-J. Werner, *J. Chem. Phys.* **103**, 2067 (1995).
- [13] K. Schreel and J. J. ter Meulen, *J. Phys. Chem. A* **101**, 7639 (1997).
- [14] H.-S. Lee, A. McCoy, R. Toczyłowski, and S. Cybulsk, *J. Chem. Phys.* **113**, 5736 (2000).
- [15] K. P. Huber and G. Herzberg, *Molecular Spectra and Molecular Structure. IV. Constants of Diatomic Molecules* (Van Nostrand Reinhold, New York, 1979).
- [16] J. Han and M. C. Heaven, *J. Chem. Phys.* **123**, 064307 (2005).
- [17] S. Marinakis, G. Paterson, J. Klos, M. L. Costen, and K. G. McKendrick, *Phys. Chem. Chem. Phys.* **9**, 4414 (2007).
- [18] J. Klos, F. Lique, and M. H. Alexander, *Chem. Phys. Lett.* **445**, 12 (2007).
- [19] G. Paterson, S. Marinakis, M. L. Costen, K. G. McKendrick, J. Klos, and R. Tobiła, *J. Chem. Phys.* **129**, 074304 (2008).
- [20] P. J. Dagdigian and M. H. Alexander, *J. Chem. Phys.* **130**, 164315 (2009).
- [21] The HIBRIDON package was written by M. H. Alexander, D. E. Manolopoulos, H.-J. Werner, and B. Follmeg, with contributions by P. F. Vohralik, D. Lemoine, G. Corey, R. Gordon, B. Johnson, T. Orlikowski, A. Berning, A. Degli-Esposti, C. Rist, P. Dagdigian, B. Pouilly, G. van der Sanden, M. Yang, F. de Weerd, S. Gregurick, and J. Klos, <http://www2.chem.umd.edu/groups/alexander/>.
- [22] B. C. Sawyer, N. K. Stuhl, D. Wang, M. Yeo, and J. Ye, *Phys. Rev. Lett.* **101**, 203203 (2008).
- [23] Z. Pavlovic, T. V. Tschernbul, H. R. Sadeghpour, G. C. Groenenboom, and A. Dalgarno, *J. Phys. Chem. A* **113**, 14670 (2009).
- [24] M. Kirste, L. Scharfenberg, J. Klos, F. Lique, M. H. Alexander, G. Meijer, and S. Y. T. van de Meerakker, *Phys. Rev. A* **82**, 042717 (2010).
- [25] K. B. Gubbels, Q. Ma, M. H. Alexander, P. J. Dagdigian, D. Tanis, G. C. Groenenboom, A. van der Avoird, and S. Y. T. van de Meerakker, *J. Chem. Phys.* **136**, 144308 (2012).
- [26] P. Jankowski and K. Szalewicz, *J. Chem. Phys.* **123**, 104301 (2005).
- [27] P. J. Dagdigian and M. H. Alexander, *J. Chem. Phys.* **137**, 094306 (2012).
- [28] A. V. Ivanov, S. Trakhtenberg, A. K. Bertram, Y. M. Gershenzon, and M. J. Molina, *J. Phys. Chem. A* **111**, 1632 (2007).
- [29] Y. Liu, A. V. Ivanov, and M. J. Molina, *Geophys. Res. Lett.* **36**, L03816 (2009).
- [30] J. M. Brown, J. Hougen, K.-P. Huber, J. Johns, I. Kopp, H. Lefebvre-Brion, A. Merer, D. Ramsay, J. Rostas, and R. Zare, *J. Molec. Spectrosc.* **55**, 500 (1975).
- [31] C. Hampel, K. A. Peterson, and H.-J. Werner, *Chem. Phys. Lett.* **190**, 1 (1992).
- [32] J. D. Watts, J. Gauss, and R. J. Bartlett, *J. Chem. Phys.* **98**, 8718 (1993).
- [33] H.-J. Werner, P. J. Knowles, G. Knizia, F. R. Manby, M. Schütz, P. Celani, T. Korona, R. Lindh, A. Mitrushenkov, G. Rauhut, K. R. Shamasundar, T. B. Adler, R. D. Amos, A. Bernhardsson, A. Berning, D. L. Cooper, M. J. O. Deegan, A. J. Dobbyn, F. Eckert, E. Goll, C. Hampel, A. Hesselmann, G. Hetzer, T. Hrenar, G. Jansen, C. Köppl, Y. Liu, A. W. Lloyd, R. A. Mata, A. J. May, S. J. McNicholas, W. Meyer, M. E. Mura, A. Nicklass, D. P. O'Neill, P. Palmieri, K. Pflüger, R. Pitzer, M. Reiher, T. Shiozaki, H. Stoll, A. J. Stone, R. Tarroni, T. Thorsteinsson, M. Wang and A. Wolf, *MOLPRO, version 2010.1*, a package of *ab initio* programs, 2010, see <http://www.molpro.net>.
- [34] S. F. Boys and F. Bernardi, *Mol. Phys.* **19**, 553 (1970).
- [35] T. H. Dunning, *J. Chem. Phys.* **90**, 1007 (1989).
- [36] K. A. Peterson, D. E. Woon, and T. H. Dunning, Jr., *J. Chem. Phys.* **100**, 7410 (1994).
- [37] H.-J. Werner and P. J. Knowles, *J. Chem. Phys.* **89**, 5803 (1988).
- [38] P. Valiron, M. Wernli, A. Faure, L. Weisenfeld, C. Rist, S. Kedžuch, and J. Noga, *J. Chem. Phys.* **129**, 134306 (2008).
- [39] D. T. Colbert and W. H. Miller, *J. Chem. Phys.* **96**, 1982 (1992).
- [40] M. Alexander, *Chem. Phys.* **92**, 337 (1985).
- [41] J. J. Gilijamse, S. Hoekstra, S. Y. T. van de Meerakker, G. C. Groenenboom, and G. Meijer, *Science* **313**, 1617 (2006).
- [42] M. A. Martin-Drumel, S. Eliet, O. Pirali, M. Guinet, F. Hindle, G. Mouret, and A. Cuisset, *Chem. Phys. Lett.* **550**, 8 (2012).
- [43] F. Lique and A. Faure, *J. Chem. Phys.* **136**, 031101 (2012).
- [44] See <http://ipag.osug.fr/Hydrides>.